Mechanics Research Communications 85 (2017) 64–68

Contents lists available at ScienceDirect

Mechanics Research Communications

journal homepage: www.elsevier.com/locate/mechrescom

Experimental slowing of flexural waves in dielectric elastomer films by voltage

Yotam Ziser, Gal Shmuel*

Faculty of Mechanical Engineering, Technion – Israel Institute of Technology, Haifa 32000, Israel

ARTICLE INFO

Article history:
Received 28 April 2017
Received in revised form 20 July 2017
Accepted 15 August 2017
Available online 24 August 2017

Keywords:
Dielectric elastomer film
Electroelasticity
Dynamics
Lamb wave
Flexural wave
Plate modes
Finite deformation

ABSTRACT

Shape and physical properties of dielectric elastomers are changeable by voltage. Theoretical works show that these changes can be harnessed to tune the propagation of superposed elastic waves. We experimentally demonstrate this concept by manipulating waves in a dielectric elastomer film, focusing on the flexural mode at low frequencies. To this end, we design an experimental apparatus to pre-stretch, actuate, excite waves at low frequencies in a VHB™ 4910 film, and measure the velocity of the fundamental flexural mode. Our results show that the excited wave velocity is slowed down by the applied voltage, and provide experimental proof of concept for the application of deformable dielectrics as tunable waveguides.

In the presence of electric fields, dielectric elastomers can experience large strains accompanied with a change in their physical properties [1,2]. The standard actuation mechanism is established by coating the surfaces perpendicular to the thickness of an elastomeric film with deformable electrodes, and connecting them to a voltage source; ensuing Coulomb forces between accumulated charge cause deformation and change the electromechanical response [3]. Various applications were realized based on this electrostatic actuation, such as tunable valves [4], noise filters [5,6], and soft robotics [7], to name just a few. (For more applications, see the book by [8].)

Recently, the potential of dielectric elastomers as tunable waveguides has been extensively explored using theory [9–18]. Corresponding experimental work—the focus of this paper—has yet to be realized, where experiments on the dynamics of soft elastomers are limited to the study of inflation [19–22] and in-plane deformation [23] of membranes, radial motions of tubes [24], and to particular actuators [25–27]. Herein, we explore the tunability of plate or *Lamb* waves [28] in a dielectric elastomer film [29]. We focus on the fundamental anti-symmetric wave—the only flexural mode in the low frequency regime. We show that the mode is slowed down by the applied voltage, as theoretically suggested [29].

1. Theory and analytical model

We begin by concisely revisiting the governing equations and analytical model; for further details the reader is referred to Refs. [30,9,29]. Consider an incompressible soft elastomeric film, whose top and bottom surfaces are coated with compliant electrodes (Fig. 1a). The film is mechanically pre-stretched such that its initial length L becomes λL. The film is constrained such that its width B is kept fixed, and since its incompressible, its initial thickness H becomes $h = H/\lambda$ (Fig. 1b). Subsequently, the film is actuated by connecting the electrodes to a voltage source of electric potential V (Fig. 1c). The resultant electric field is $\frac{V}{h}$ along x_2, where x_1 and x_2 are coordinates in the axial and thickness directions, respectively. Since the film is clamped, the actuation is not accompanied with a deformation. However, resultant Coulomb forces between opposite charges modify the electromechanical behavior of the film. This change depends on the constitutive behavior of the elastomer, which we assume described by a neo-Hookean ideal dielectric model [31]

$$\Psi(\mathbf{F},\mathbf{D}) = \frac{\mu}{2}\left(\mathbf{F}^{\mathrm{T}}\mathbf{F} - 3\right) + \frac{1}{2\epsilon}\mathbf{D}\cdot\mathbf{F}^{\mathrm{T}}\mathbf{F}\mathbf{D}; \tag{1}$$

here μ is the shear modulus, ϵ is the dielectric constant, $\mathbf{F}$ is the deformation gradient and $\mathbf{D}$ is the Lagrangian electric displacement

* Corresponding author.
E-mail address: meshmuel@tx.technion.ac.il (G. Shmuel).

http://dx.doi.org/10.1016/j.mechrescom.2017.08.005
0093-6413/

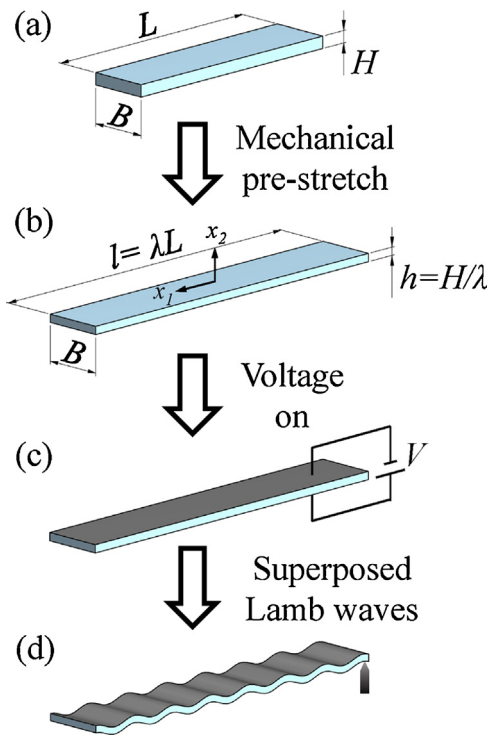

Fig. 1. An elastomeric film coated with compliant electrodes (a) in the reference configuration; (b) clamped after pre-stretched, (c) subjected to a voltage V and (d) when Lamb waves are excited on top of its actuated state.

field [30]. Owing to harmonic excitation on top of the actuated state, small-amplitude elastic waves propagate in the longitudinal direction (Fig. 1d). To determine these time-dependent displacements $\mathbf{u}(\mathbf{x}, t)$ and resultant change in the electric fields, the following equations are solved

$$\nabla \cdot \boldsymbol{\Sigma} = \rho \mathbf{u}_{,tt}, \quad \nabla \cdot \check{\mathbf{d}} = 0, \quad \nabla \times \check{\mathbf{e}} = \mathbf{0}, \tag{2}$$

where $\boldsymbol{\Sigma}$, $\check{\mathbf{d}}$ and $\check{\mathbf{e}}$ are increments in the Lagrangian stress, electric displacement and electric fields, respectively, expressed in terms of the coordinates x_i. These fields are related by the following linearization of the constitutive model about the deformed state

$$\Sigma_{ij} = \mathcal{C}_{ijkl} u_{i,j} + p_0 u_{j,i} - \dot{p}_0 \delta_{ij} + \mathcal{B}_{ijk} \check{d}_k, \check{e}_i = \mathcal{B}_{jki} h_{jk} + \mathcal{A}_{ij} \check{d}_j, \tag{3}$$

where $\dot{p}_0$ is the increment of the Lagrange multiplier p_0, and the non-zero components of the instantaneous moduli in our settings are

$$\mathcal{A}_{11} = \mathcal{A}_{22} = \frac{1}{\epsilon}, \quad \mathcal{B}_{121} = \mathcal{B}_{211} = \frac{1}{2}\mathcal{B}_{222} = \frac{V}{h}, \tag{4}$$

$$\mathcal{C}_{1111} = \mathcal{C}_{1212} = \mathcal{C}_{2121} = \mu\lambda^2, \quad \mathcal{C}_{1212} = \mathcal{C}_{2222} = \frac{\mu}{\lambda^2} + \epsilon\frac{V^2}{h^2}. \tag{5}$$

The bias electric field affects the dynamic response through the components $\mathcal{C}_{1212}$ and $\mathcal{C}_{2222}$ and the coupling tensor $\boldsymbol{B}$. We seek solutions for the unknowns $\mathbf{u}$ and $\check{\mathbf{d}}$ in the form

$$u_1 = \phi_{,2}, \quad u_2 = -\phi_{,1}, \quad \check{d}_1 = \varphi_{,2}, \quad \check{d}_2 = -\varphi_{,1}. \tag{6}$$

where $\phi = Ae^{kqx_2}e^{ik(x_1-ct)}$ and $\varphi = kBe^{kqx_2}e^{ik(x_1-ct)}$, such that $\nabla \cdot \check{\mathbf{d}} = 0$ and the incompressibility constraint $\nabla \cdot \mathbf{u} = 0$ are identically satisfied. Here, A and B are the amplitudes, k is the wavenumber, c is the phase velocity, and the excitation frequency ω equals ck. Eqs. (3) and (6) are substituted into the first and last of Eq. (2). After some manipulation, a vanishing condition on the resultant determinant of the coefficients of A and B provides solutions for q [29], where each solution q_i is associated with amplitudes A_i and B_i. Finally, the *dispersion relation* between c and k is obtained by substituting these solutions into the boundary conditions at the top and bottom surfaces

$$\Sigma_{12} = \Sigma_{22} = \check{e}_1 = 0 \text{ at } x_2 = \pm\frac{h}{2}, \tag{7}$$

and equating the determinant of the coefficients of the amplitudes to zero. Note that here we consider a prescribed fixed voltage to the electrodes, hence the external fields vanish, and the boundary conditions obtain the above form. As in Ref. [29], the velocity of fundamental anti-symmetric mode (A_0), corresponding to a flexural wave, is found to be slowed down by the applied voltage. Our objective is to provide an experimental observation of this phenomenon.

2. Experimental setup

The experimental apparatus (Fig. 2) consists of a customized mechanical setup in our lab, designed to carry out the following tasks:

i. Pre-stretching and clamping the film in the axial direction, while maintaining its width fixed. The objective is to approximate the plane-strain nature of the underlaying deformation considered, where the finite deformation is only in the axial and thickness directions. To this end, we clamp the edges in the transverse direction of the layer with ball bearings.
ii. Coating carbon grease electrodes on the surfaces of the stretched film.
iii. Applying voltage through copper tape terminals to the carbon grease electrodes.
iv. Exciting and measuring elastic waves, as we describe next in detail.

The film is electrically excited by a high voltage supply (Spellman type SL10), capable of delivering an output voltage up to 10 kV. The sinusoidal excitation signal is generated by a TTI TG2000 function generator. The signal is amplified with a Bruel Kjaer type 4809 amplifier and delivered by a Bruel Kjaer type 4809 shaker. Two accelerometers (TE 805M1 series) are attached to the rods, in order to measure of the input and output signals. The accelerometers are connected to a digital oscilloscope (Agilent Technologies, type DSO-X 3024A) which stores the signals. The signals are transferred to a PC for further processing in Matlab®.

We excite plate modes utilizing a spherical contact between an input rod and the film. This approach is suitable to comply with the soft nature of the film, as its success in a series of experiments on silicone wafers demonstrates [32,33]. The working principle is as follows. A shaker generates longitudinal waves through an input rod, perpendicular to the surface of the film, as illustrated in Fig. 2a. In turn, these longitudinal waves excite Lamb waves in the film, emanating from the contact between the rod and the film. Since the contact is on one side of the film, only anti-symmetric modes are excited [33]. Specifically, at low values of the product between the frequency and the thickness of the film, the only propagating Lamb mode is the fundamental lowest order—A_0. The mode propagates in the film to an output rod which oscillates accordingly. The wave velocity c is extracted by measuring the propagation distance Δx and dividing it by the Time Of Flight (TOF) Δt between the input and output signals. The propagation distance is measured with a caliper, and we measure the same distance throughout the experiments. The calculation is demonstrated in Fig. 3, in which the normalized acceleration is displayed as a function of time. The continuous and dashed curves correspond to the input and output signals, respectively.

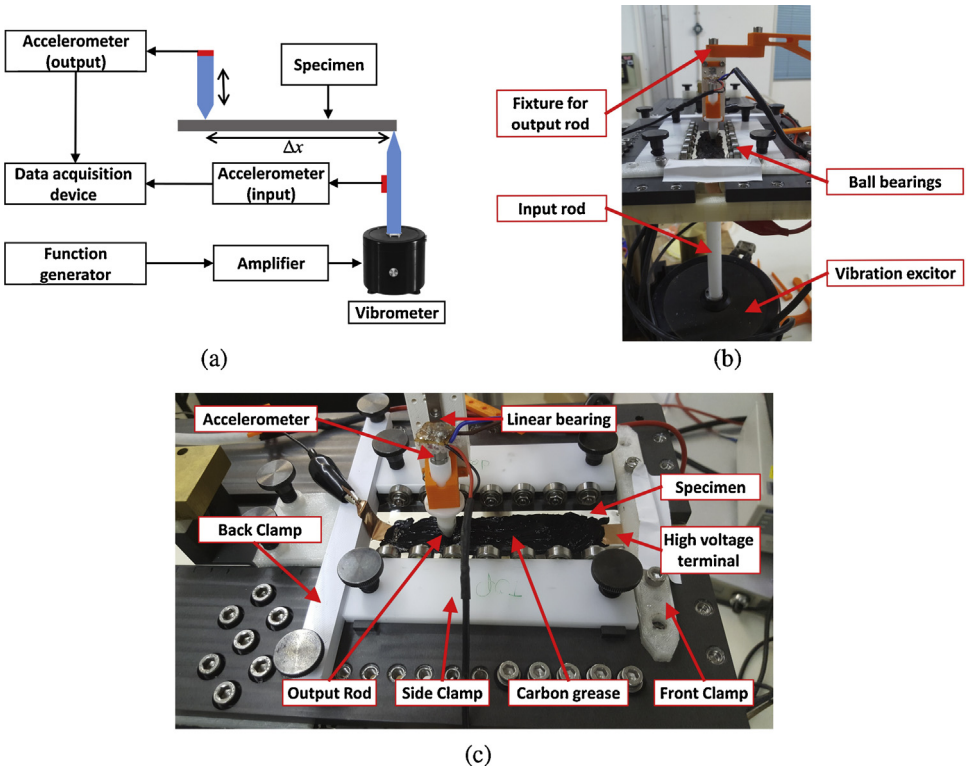

Fig. 2. Experiment outline: (a) A schematic overview of experiment setup. (b) Side view of the experiment setup. (c) Top view of the experiment setup.

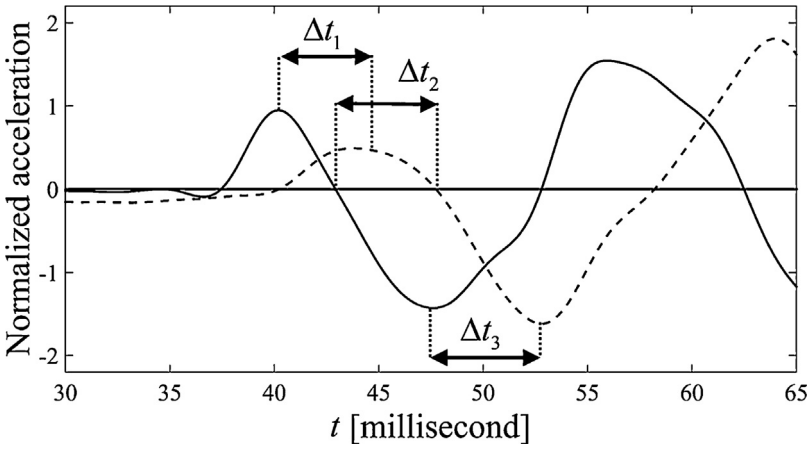

Fig. 3. Exemplary TOF calculation. The normalized acceleration is displayed as function of time. The continuous and dashed curves correspond to the input and output signals, respectively. The segments Δt_1, Δt_2 and Δt_3 correspond to the TOF between peaks, vanishing acceleration and lows of the input and output signal, respectively.

The contact rods are manufactured with a polished spherical tip to achieve a Point Source-Point Receiver (PS-PR) contact. This type of contact is required in order to accurately measure the propagation distance. The criterion for the PS-PR contact is that the wavelength should be larger by at least an order of magnitude than the resultant surface radius contact.

Note that waves reflected from the transverse boundaries of the film interfere with the Lamb mode, since the film is not sufficiently wide to avoid this interference. To eliminate the influence of the reflections on the data, the TOF measurements are conducted at early time instances, before the measured signal is affected by the reflections. The velocity at each frequency contains a random error of $\pm 0.5\,\mathrm{m\,s^{-1}}$, based on repeatability measurements conducted on a specimen pre-stretched to $\lambda = 4$. The error is independent of the applied voltage.

Tests were conducted across the frequency range 0–200 Hz, in increments of 10 Hz. Magnitudes of voltages up to 5 kV were applied. Beyond that voltage, the film experienced *electric breakdown*, during which it loses its insulating property [34].

3. Results and discussion

Firstly, experimental results of the wave velocity c as function of the wavenumber k are presented in Fig. 4, when a representative voltage of 2 kV is applied on top of two different stretch states. Specifically, the triangle and square marks correspond to the experimental measurements when the underlaying stretch is $\lambda = 1$ (the film is clamped in its initial configuration) and when $\lambda = 4$, respectively. The continuous and dashed lines correspond to the linear fit of the experimental data at $\lambda = 1$ and $\lambda = 4$, respectively. The disper-

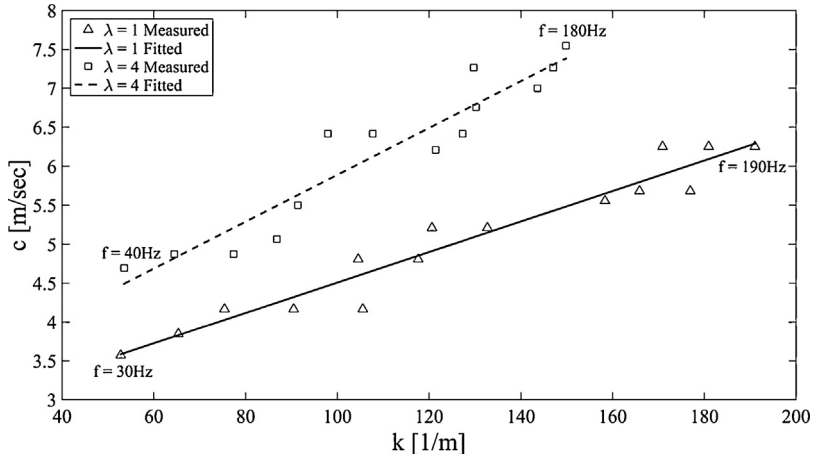

Fig. 4. Experimental results of the wave velocity c as function of the wavenumber k, when a representative voltage of 2 kV is applied on top of two different stretch states. The triangle and square marks correspond to the experimental measurements at the stretches $\lambda = 1$ and $\lambda = 4$, respectively. The continuous and dashed lines correspond to the linear fit of the experimental data at $\lambda = 1$ and $\lambda = 4$, respectively. The frequencies at which the first and last marks were measured are specified next to these marks.

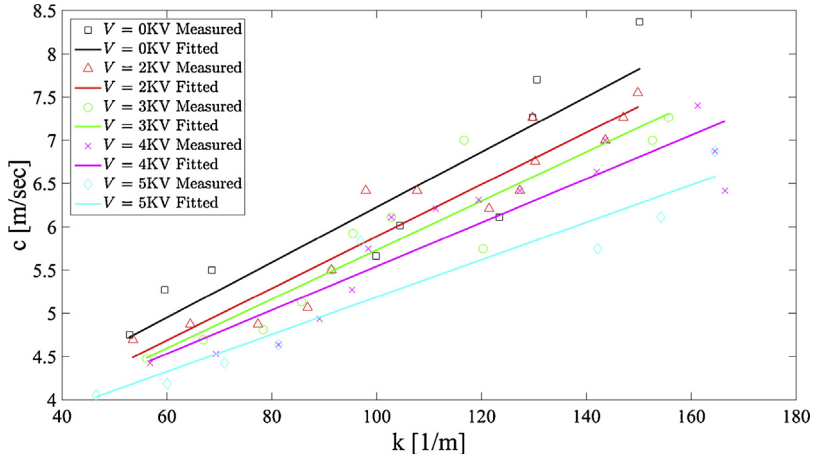

Fig. 5. Experimental results of the wave velocity c as function of the wavenumber k, at $\lambda = 4$ and different magnitudes of voltage. Specifically, the square, triangle, circle, cross and diamond markers correspond to experimental measurements at $V = 0$, 2, 3, 4 and 5 kV, respectively. The black, red, green, magenta and cyan lines correspond to their linear fits, respectively. (For interpretation of the references to color in this figure legend, the reader is referred to the web version of the article.)

sion curves are obtained across a narrow range of wavelengths (low frequencies), and therefore demonstrate a linear trend. At these low frequencies, the velocity is higher when the actuated film is pre-stretched, in agreement with the theoretical predictions [29], similarly to the purely elastic case [35,36].

Experimental results of the wave velocity c as function of the wavenumber k at different magnitudes of voltage are presented next. Specifically, the square, triangle, circle, cross and diamond markers in Fig. 5 correspond to experimental measurements when the magnitudes $V = 0$, 2, 3, 4 and 5 kV are applied at the stretch $\lambda = 4$, respectively. The black, red, green, magenta and cyan lines correspond to their linear fits, respectively. We observe that the wave velocity decreases with increasing magnitude of voltage. This trend is qualitatively in agreement with theoretical predictions.

4. Conclusions

We have established an experimental apparatus to pre-stretch, actuate, and excite the fundamental flexural Lamb mode in a dielectric elastomer film at low frequencies. From experimental measurements, we have calculated the wave velocity when the film is clamped in its initial configuration and when pre-stretched, under different magnitudes of voltage. The velocity at the examined frequencies in an actuated pre-stretched film is higher than in a film that was actuated by the same voltage, without being stretched. Thus, actuating the film does not change this effect stretching has demonstrated in the purely elastic setting. Importantly, measurements from films which were identically pre-stretched, while subjected to different magnitudes of voltages, show that at low frequencies the wave velocity is slowed down by voltage. Our results provide experimental proof of concept for the application of deformable dielectrics as tunable waveguides.

Acknowledgments

We gratefully acknowledge the support of the Israel Science Foundation, funded by the Israel Academy of Sciences and Humanities (Grant no. 1912/15), the United States-Israel Binational Science Foundation (Grant no. 2014358). We also thank Prof. Doron Shilo for valuable advice, and Prof. Oded Gottlieb for lended equipment.

References

[1] X. Zhao, Z. Suo, Theory of dielectric elastomers capable of giant deformation of actuation, Phys. Rev. Lett. 104 (17) (2010) 178302.
[2] N. Cohen, G. deBotton, Electromechanical interplay in deformable dielectric elastomer networks, Phys. Rev. Lett. 116 (May) (2016) 208303.
[3] R. Pelrine, R. Kornbluh, Q.-B. Pei, J. Joseph, High-speed electrically actuated elastomers with strain greater than 100%, Science 287 (2000) 836–839.

[4] D. McCoul, Q. Pei, Tubular dielectric elastomer actuator for active fluidic control, Smart Mater. Struct. 24 (10) (2015) 105016.
[5] K. Jia, M. Wang, T. Lu, J. Zhang, T. Wang, Band-gap tunable dielectric elastomer filter for low frequency noise, Smart Mater. Struct. 25 (5) (2016) 055047.
[6] X. Yu, Z. Lu, F. Cui, L. Cheng, Y. Cui, Tunable acoustic metamaterial with an array of resonators actuated by dielectric elastomer, Extreme Mech. Lett. 12 (2017) 37–40 (Frontiers in Mechanical Metamaterials).
[7] G.-Y. Gu, J. Zhu, L.-M. Zhu, X. Zhu, A survey on dielectric elastomer actuators for soft robots, Bioinspir. Biomim. 12 (1) (2017) 011003.
[8] F. Carpi, D. De Rossi, R. Kornbluh, R. Pelrine, P. Sommer-Larsen, Dielectric Elastomers as Electromechanical Transducers: Fundamentals, Materials, Devices, Models and Applications of an Emerging Electroactive Polymer Technology, Elsevier Science, 2008.
[9] A. Dorfmann, R.W. Ogden, Electroelastic waves in a finitely deformed electroactive material, IMA J. Appl. Math. 75 (2010) 603–636.
[10] M. Gei, S. Roccabianca, M. Bacca, Controlling bandgap in electroactive polymer-based structures, IEEE-ASME Trans. Mechatron. 16 (2011) 102–107.
[11] G. Shmuel, G. deBotton, Band-gaps in electrostatically controlled dielectric laminates subjected to incremental shear motions, J. Mech. Phys. Solids 60 (2012) 1970–1981.
[12] G. Shmuel, Manipulating torsional motions of soft dielectric tubes, J. Appl. Phys. 117 (17) (2015).
[13] Y.Z. Wang, C.L. Zhang, H.-H. Dai, W.Q. Chen, Adjustable solitary waves in electroactive rods, J. Sound Vib. 355 (2015) 188–207.
[14] R. Getz, D.M. Kochmann, G. Shmuel, Voltage-controlled complete stopbands in two-dimensional soft dielectrics, Int. J. Solids Struct. 113–114 (2017) 24–36.
[15] Y. Su, W. Zhou, W. Chen, C. Lü, On buckling of a soft incompressible electroactive hollow cylinder, Int. J. Solids Struct. 97–98 (2016) 400–416.
[16] G. Shmuel, R. Pernas-Salomón, Manipulating motions of elastomer films by electrostatically-controlled aperiodicity, Smart Mater. Struct. 25 (12) (2016) 125012.
[17] B. Wu, Y. Su, W. Chen, C. Zhang, On guided circumferential waves in soft electroactive tubes under radially inhomogeneous biasing fields, J. Mech. Phys. Solids 99 (2017) 116–145.
[18] E. Bortot, G. Shmuel, Tuning sound with soft dielectrics, Smart Mater. Struct. 26 (2017) 045028.
[19] J.W. Fox, N.C. Goulbourne, On the dynamic electromechanical loading of dielectric elastomer membranes, J. Mech. Phys. Solids 56 (8) (2008) 2669–2686.
[20] J.W. Fox, N.C. Goulbourne, Electric field-induced surface transformations and experimental dynamic characteristics of dielectric elastomer membranes, J. Mech. Phys. Solids 57 (8) (2009) 1417–1435.
[21] K. Hochradel, S.J. Rupitsch, A. Sutor, R. Lerch, D.K. Vu, P. Steinmann, Dynamic performance of dielectric elastomers utilized as acoustic actuators, Appl. Phys. A 107 (3) (2012) 531–538.
[22] S. Sasikala, K.T. Madhavan, G. Ramesh, S. Saggar, P. Predeep, P. Chowdhury, Electro-mechanical response to the harmonic actuation of the pneumatically coupled dielectric elastomer based actuators with and without load, Int. J. Solids Struct. 110–111 (2017) 58–66.
[23] L. Liu, H. Chen, J. Sheng, J. Zhang, Y. Wang, S. Jia, Experimental study on the dynamic response of in-plane deformation of dielectric elastomer under alternating electric load, Smart Mater. Struct. 23 (2) (2014).
[24] S. Son, N.C. Goulbourne, Dynamic response of tubular dielectric elastomer transducers, Int. J. Solids Struct. 47 (20) (2010) 2672–2679.
[25] R. Sarban, B. Lassen, M. Willatzen, Dynamic electromechanical modeling of dielectric elastomer actuators with metallic electrodes, IEEE/ASME Trans. Mechatron. 17 (October (5)) (2012) 960–967.
[26] G. Berselli, R. Vertechy, M. BabiLtdc:č:rtdc, V.P. Castelli, Dynamic modeling and experimental evaluation of a constant-force dielectric elastomer actuator, J. Intell. Mater. Syst. Struct. 24 (6) (2013) 779–791.
[27] M. Hodgins, G. Rizzello, D. Naso, A. York, S. Seelecke, An electro-mechanically coupled model for the dynamic behavior of a dielectric electro-active polymer actuator, Smart Mater. Struct. 23 (10) (2014) 104006.
[28] H. Lamb, On waves in an elastic plate, Proc. R. Soc. Lond. Ser. A A93 (1917) 114–128.
[29] G. Shmuel, M. Gei, G. deBotton, The Rayleigh–Lamb wave propagation in dielectric elastomer layers subjected to large deformations, Int. J. Non-Linear Mech. 47 (2) (2012) 307–316.
[30] A. Dorfmann, R.W. Ogden, Nonlinear electroelasticity, Acta Mech. 174 (2005) 167–183.
[31] X. Zhao, Q. Wang, Harnessing large deformation and instabilities of soft dielectrics: theory, experiment, and application, Appl. Phys. Rev. 1 (2) (2014) 021304.
[32] F.L. Degertekin, B.T. Khuri-Yakub, Single mode lamb wave excitation in thin plates by Hertzian contacts, Appl. Phys. Lett. (1996).
[33] F.L. Degertakin, B. Khuri-Yakub, Lamb wave excitation by Hertzian contacts with applications in NDE, IEEE Trans. Ultrason. Ferroelectr. Freq. Control 44 (July (4)) (1997) 769–779.
[34] J.S. Plante, S. Dubowsky, Large-scale failure modes of dielectric elastomer actuators, Int. J. Solids Struct. 43 (25–26) (2006) 7727–7751.
[35] R.W. Ogden, D.G. Roxburgh, The effect of pre-stress on the vibration and stability of elastic plates, Int. J. Eng. Sci. 31 (12) (1993) 1611–1639.
[36] M. Mohabuth, A. Kotousov, C.-T. Ng, Effect of uniaxial stress on the propagation of higher-order lamb wave modes, Int. J. Non-Linear Mech. 86 (2016) 104–111.